ICNDT 2026 Conference

The 1st International Online Conference on Non-Destructive Testing

1–3 July 2026 | Online

MDPI

Waveguide effects in structural GPR data: Numerical Insights

Davide Campo

Independent Researcher, London, United Kingdom

Orcid: 0000-0002-5261-4376

INTRODUCTION

In high frequency common-offset GPR surveys, horizontal signal signatures are often misidentified as mere artifacts rather than lateral wave components and guided wave modes.

Layered structural elements can act as waveguides (or more in general they can favour lateral propagation) extending the radar sensing capabilities far beyond the conventional vertical line of sight and allowing for alternative ways of velocity estimation.

This study explores the physical mechanisms triggering lateral wave propagation by combining numerical modelling with real data.

Theoretical Background And Numerical Modelling

In a simplified layered structure where a lower-velocity medium is bounded by higher-velocity materials (i.e., a suspended concrete slab), the thickness-to-wavelength ratio (*d/λ*) governs the wave propagation regime.

$$\frac{d}{\lambda} > 1 \quad \rightarrow \quad \frac{d}{\lambda} < 1$$

Bulk Propagation Regime (individual wave phases)

Guided-wave Regime (dispersive patterns)

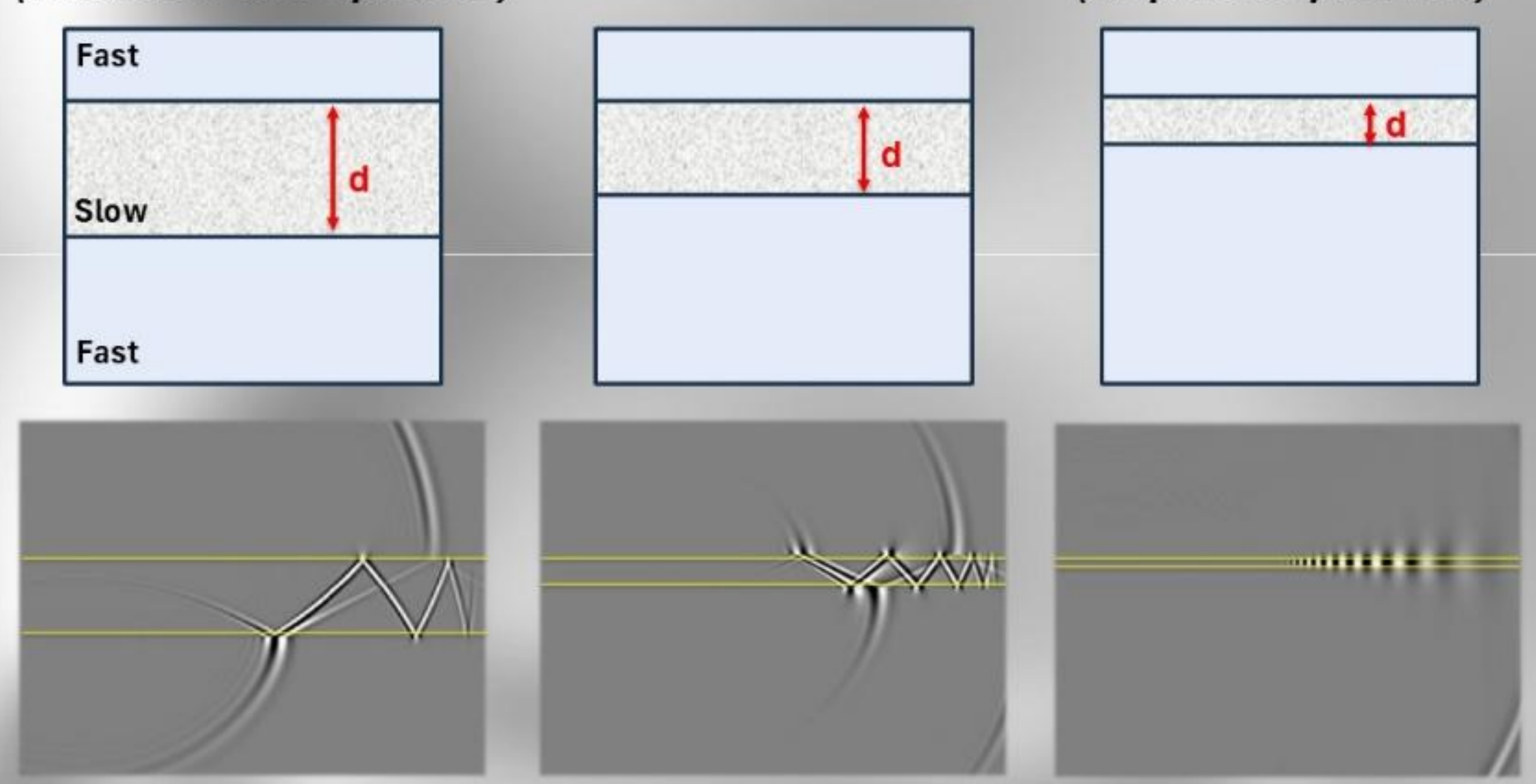

As the ratio decreases, the individual lateral wave components (bulk regime) tend to converge and merge until they can no longer be distinguished (waveguide regime). These behaviours can be observed in multi-offset (left) and common-offset (right) data, though the latter requires a diffraction point to make the horizontal component detectable.

Multi-offset synthetic data | ***Common-offset synthetic data***

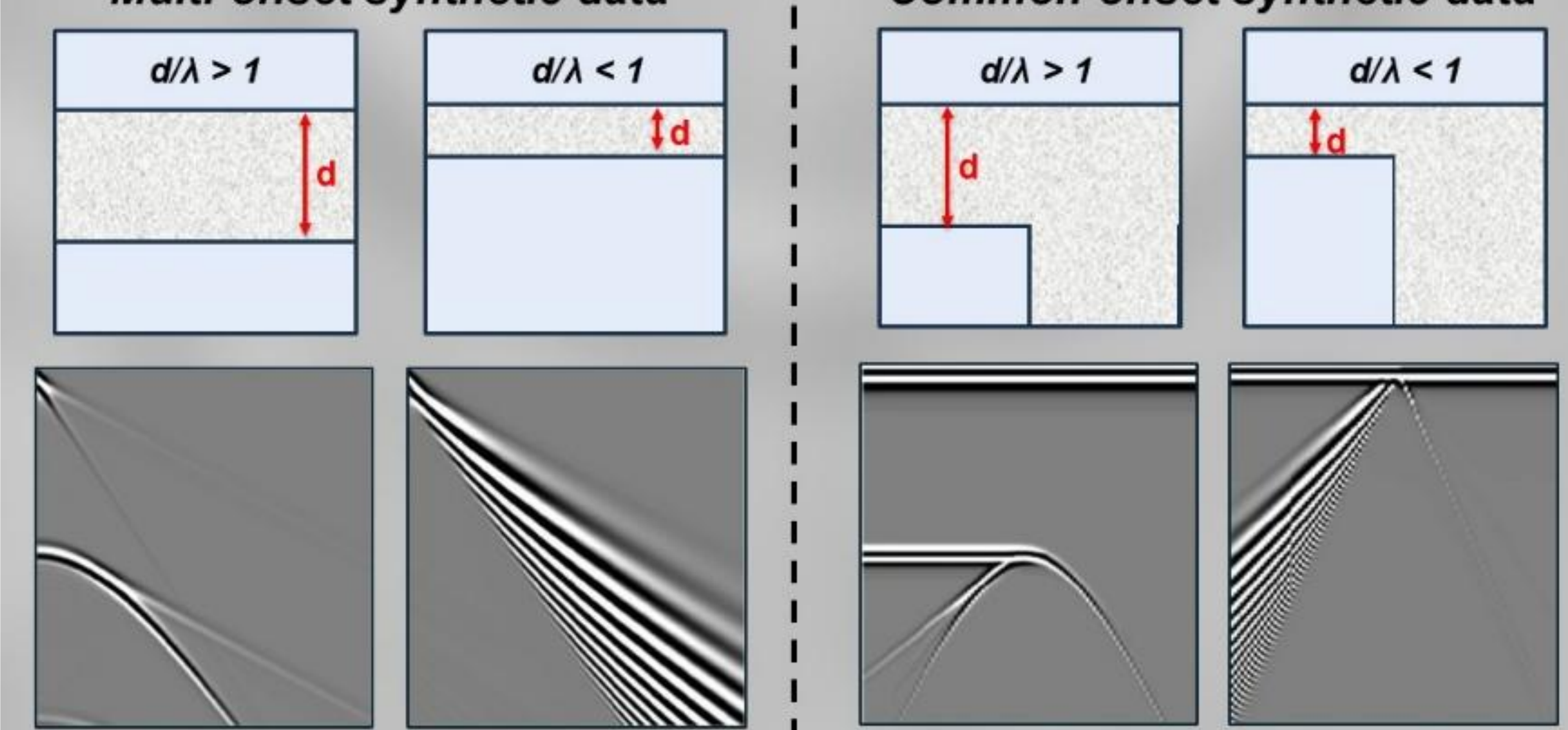

Case Study 1: Masonry Arch Supported By Steel Beams

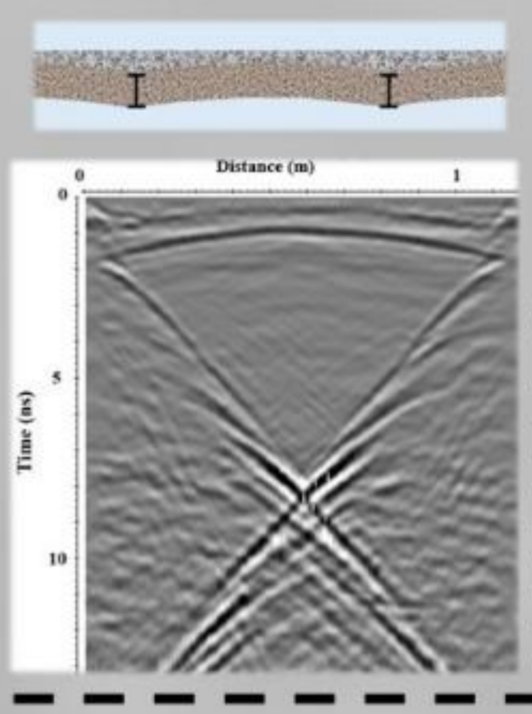

In addition to expected signals from the arch intrados, extrados, and beams, the data exhibit prominent shingled patterns typically associated with guided waves

Numerical modelling confirms that the arch structure acts as a waveguide. The lateral wave components are only visible near steel beams, which act as structural discontinuities that reflect energy back to the antenna.

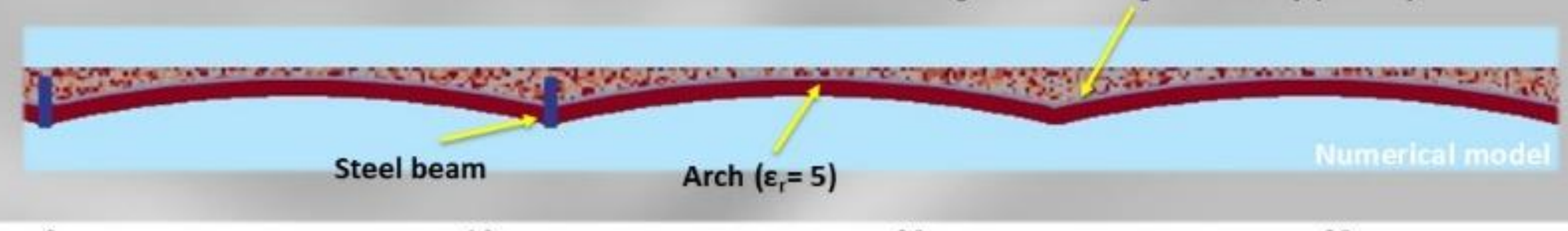

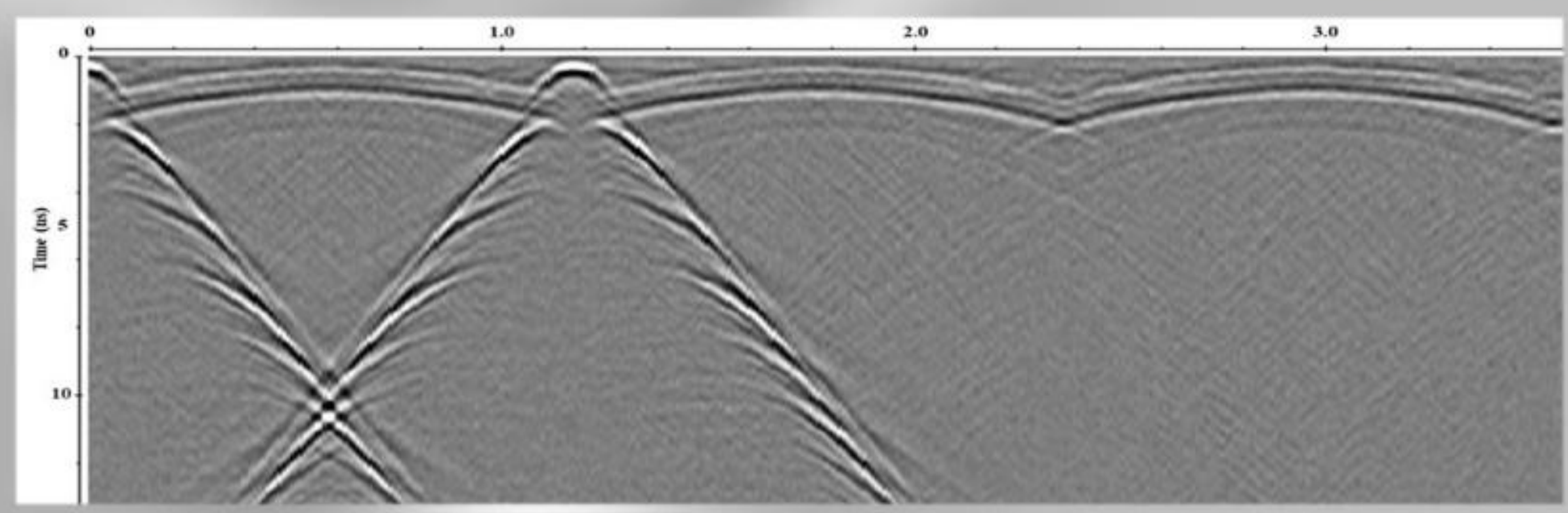

Case study 2: Mass Concrete Slab and Expansion Joints

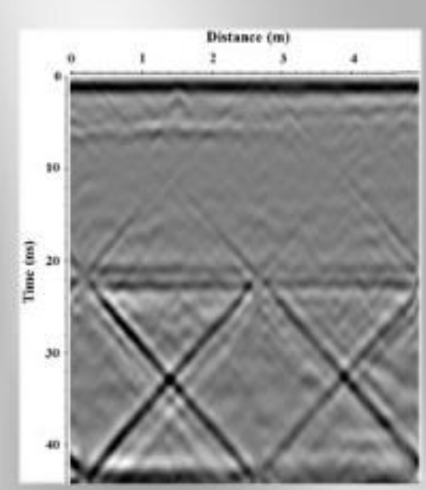

Scans collected parallel to and centimetres away from metallic expansion joints show prominent x-patterns (high amplitude in the real data on the left is due to gain amplification at depth).

Numerical modelling of shallow metallic linear elements in a dielectric half-space confirms that the parallel joint acts as waveguide forcing the energy to travel along the joint until it is reflected by an intersecting joint.

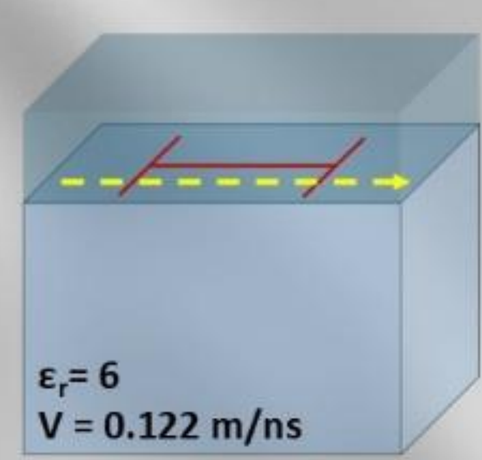

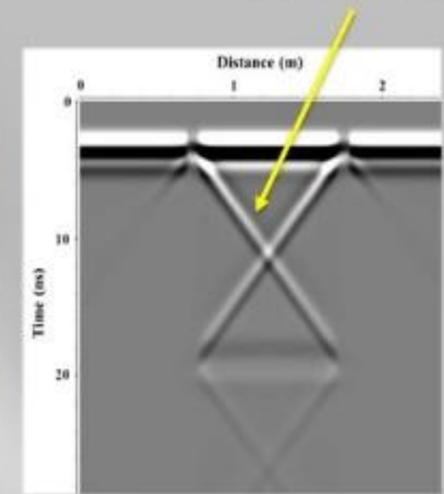

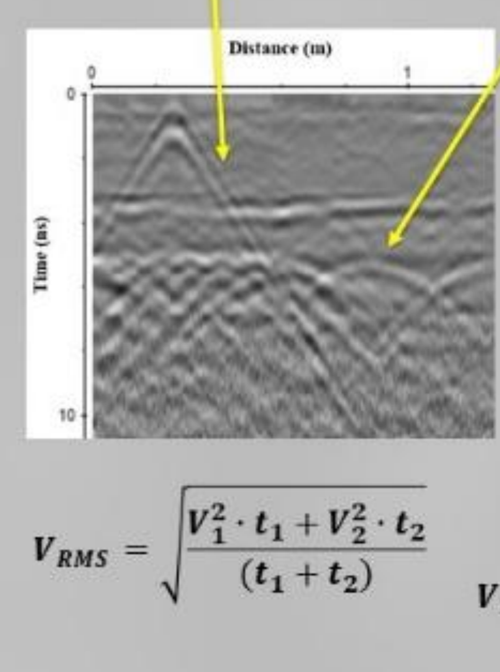

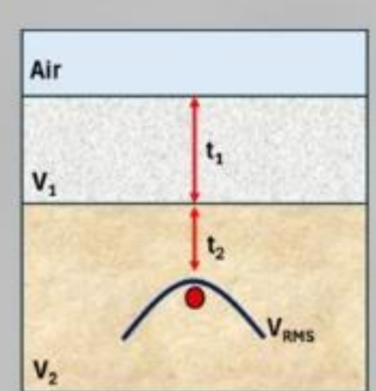

$$V_{RMS} = \sqrt{\frac{V_1^2 \cdot t_1 + V_2^2 \cdot t_2}{(t_1 + t_2)}} \qquad V_2 = \sqrt{\frac{V_1^2 \cdot t_1 + V_{RMS}^2 \cdot (t_1 + t_2)}{t_2}}$$

Being it a linear travel path, the angular coefficient of a linear pattern is the inverse of half of the top layer velocity.

Linear (for V_1) and hyperbolic fitting (for V_{RMS}) can be used synergically in a two-layer structure to determine the interval velocity V_2.

CONCLUSIONS

Two case studies were analysed using numerical modelling identify the origin of distinct patterns in common-offset data. Results link these patterns to significant lateral wave components.

Under favourable conditions, these patterns can provide enhanced side-sight capability, especially in restricted access locations (case study 1), or insights about the top layer velocity (case study 2) via linear fitting.

Acknowledgements:
the author thanks Sandberg LLP for having shared the use of part of their dataset.